THE JOURNAL OF PHYSICAL CHEMISTRY A

ARTICLE

pubs.acs.org/JPCA

Atmospheric Chemistry of Dichlorvos

Sara M. Aschmann,[†] Ernesto C. Tuazon,[†] William D. Long,[†] and Roger Atkinson*[,†,‡,§]

[†]Air Pollution Research Center, [‡]Department of Environmental Sciences, and [§]Department of Chemistry, University of California, Riverside, California 92521, United States

ABSTRACT: Dichlorvos [2,2-dichlorovinyl dimethyl phosphate, $(CH_3O)_2P(O)OCH{=}CCl_2$] is a relatively volatile in-use insecticide. Rate constants for its reaction with OH radicals have been measured over the temperature range 296−348 K and atmospheric pressure of air using a relative rate method. The rate expression obtained was $3.53 \times 10^{-13}\ e^{(1367\pm239)/T}$ cm^3 molecule^{-1} s^{-1}, with a 298 K rate constant of $(3.5 \pm 0.7) \times 10^{-11}$ cm^3 molecule^{-1} s^{-1}, where the error in the 298 K rate constant is the estimated overall uncertainty. In addition, rate constants for the reactions of NO_3 radicals and O_3 with dichlorvos, of $(2.5 \pm 0.5) \times 10^{-13}$ cm^3 molecule^{-1} s^{-1} and $(1.7 \pm 1.0) \times 10^{-19}$ cm^3 molecule^{-1} s^{-1}, respectively, were measured at 296 ± 2 K. Products of the OH and NO_3 radical-initiated reactions were investigated using in situ atmospheric pressure ionization mass spectrometry (API-MS) and (OH radical reaction only) in situ Fourier transform infrared (FT-IR) spectroscopy. For the OH radical reaction, the major initial products were CO, phosgene [$C(O)Cl_2$] and dimethyl phosphate [$(CH_3O)_2P(O)OH$], with equal (to within ±10%) formation yields of CO and $C(O)Cl_2$. The API-MS analyses were consistent with formation of $(CH_3O)_2P(O)OH$ from both the OH and NO_3 radical-initiated reactions. In the atmosphere, the dominant chemical loss processes for dichlorvos will be daytime reaction with OH radicals and nighttime reaction with NO_3 radicals, with an estimated lifetime of a few hours.

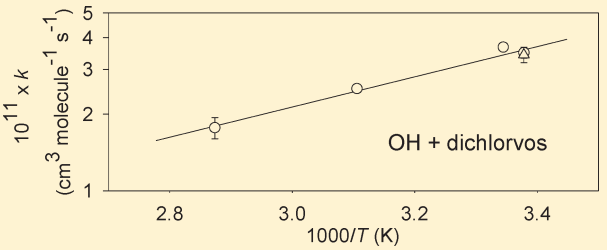

INTRODUCTION

Volatile organic compounds emitted into the troposphere can be chemically transformed by photolysis (at wavelengths >290 nm) and reactions with OH radicals, NO_3 radicals, O_3, and Cl atoms.[1] Organophosphorus compounds are widely used as pesticides,[2] and can be released into the atmosphere where they can undergo transport and chemical reactions. Rate constants for the gas-phase reactions of a number of organophosphorus compounds of structure $(RO)_nP(X)(SR)_{3-n}$ and $(RO)_2P(X)Y$, where R = CH_3, C_2H_5, or $CH(CH_3)_2$, X = O or S, and Y = H, CH_3, C_2H_5, NH_2, $NHCH_3$, $N(CH_3)_2$, $OCH{=}CCl_2$, and Cl, with OH radicals, NO_3 radicals and O_3 have been reported.[3−16] For those organophosphorus compounds for which data are available, reaction with OH radicals is calculated to dominate in the atmosphere.[4,5,8,10,13,16]

The majority of the organophosphorus compounds studied to date have been simple model compounds chosen to investigate the effects of structure on their reactivities. The only in-use organophosphorus pesticide studied to date is dichlorvos [2,2-dichlorovinyl dimethyl phosphate, $(CH_3O)_2P(O)OCH{=}CCl_2$], a relatively volatile insecticide with a vapor pressure of 5×10^{-2} Torr at 298 K[17] and a reported usage in the USA in 1989 of 992 000 lb.[18] Rate constants for the reaction of OH radicals with dichlorvos have been measured at room temperature,[9,11] and the products of the OH radical-initiated reaction investigated.[11] In addition, Zhang et al.[19] have reported a theoretical study of potential initial and subsequent reaction pathways for its OH radical-initiated reaction. In this work, we have investigated the kinetics and products of the reactions of dichlorvos with OH and NO_3 radicals, including measuring the OH radical reaction rate constants over the temperature range 296−348 K. In addition, a room temperature rate constant for the reaction of dichlorvos with O_3 has been measured.

EXPERIMENTAL METHODS

Experiments at room temperature and atmospheric pressure (∼735 Torr), other than those employing in situ Fourier transform infrared (FT-IR) spectroscopy (see below), were carried out in two ∼7000 L Teflon chambers, each equipped with two parallel banks of blacklamps for irradiation. One of these Teflon chambers is interfaced to a PE SCIEX API III MS/MS direct air sampling atmospheric pressure ionization tandem mass spectrometer (API-MS). Experiments utilizing in situ FT-IR spectroscopy were carried out at 298 ± 2 K and 740 Torr total pressure of synthetic air (80% N_2 + 20% O_2) in a 5870 L Teflon-coated, evacuable chamber equipped with a multiple reflection optical system interfaced to a Mattson Galaxy 5020 FT-IR spectrometer,[8,10] and with irradiation being provided by a 24-kW xenon arc lamp at wavelengths >300 nm. Temperature-dependent experiments were carried out at atmospheric pressure with a ∼5000 L Teflon bag inserted inside the 5870 L chamber,[12] which is fitted with a heating/cooling system allowing its temperature to be maintained to within ±1 K over the range ∼280−350 K. All of the chambers have Teflon-coated fans to ensure rapid mixing of reactants during their introduction into the chamber.

Received: December 17, 2010
Revised: February 9, 2011
Published: March 15, 2011

Kinetic Studies. Rate constants for the reactions of OH and NO_3 radicals with dichlorvos were measured using relative rate techniques in which the concentrations of dichlorvos and a reference compound (whose OH or NO_3 radical reaction rate constant is reliably known) were measured in the presence of OH or NO_3 radicals.

$$\left.\begin{matrix}\text{OH}\\ \text{NO}_3\end{matrix}\right\} + \text{dichlorvos} \rightarrow \text{products} \qquad (1)$$

$$\left.\begin{matrix}\text{OH}\\ \text{NO}_3\end{matrix}\right\} + \text{reference compound} \rightarrow \text{products} \qquad (2)$$

In addition, dichlorvos can be removed from the gas-phase by losses at the chamber walls, at a rate k_w. Providing that dichlorvos and the reference compound reacted only with OH radicals or NO_3 radicals, then,

$$\ln\left(\frac{[\text{dichlorvos}]_{t_o}}{[\text{dichlorvos}]_t}\right) - k_w(t_o - t) - D_t = \frac{k_1}{k_2}\left[\ln\left(\frac{[\text{reference compound}]_{t_o}}{[\text{reference compound}]_t}\right) - D_t\right] \qquad (I)$$

where $[\text{dichlorvos}]_{t_o}$ and $[\text{reference compound}]_{t_o}$ are the concentrations of dichlorvos and reference compound, respectively, at time t_o, $[\text{dichlorvos}]_t$ and $[\text{reference compound}]_t$ are the corresponding concentrations at time t, k_w is the dichlorvos wall loss rate, D_t is a factor to account for dilution caused by any additions to the chamber during the experiments ($D_t = 0$ for the OH radical reactions and $D_t = 0.0027$ per N_2O_5 addition to the ~7000 L volume chamber in the NO_3 radical reactions), and k_1 and k_2 are the rate constants for reactions 1 and 2, respectively.

Hydroxyl radicals were generated in the presence of NO by the photolysis of CH_3ONO at wavelengths >300 nm, with initial reactant concentrations (molecules cm^{-3}) of: CH_3ONO, ~2.4×10^{14}; NO, ~2.4×10^{14}; and dichlorvos and reference compound, ~2.4×10^{13} each. Ethane, at a concentration of $(2.7-3.2) \times 10^{15}$ molecules cm^{-3}, was added in certain experiments to scavenge any Cl atoms generated. Experiments were also conducted to investigate the importance of dark decay and photolysis of dichlorvos (~2.4×10^{13} molecules cm^{-3}) in the chamber, with 2.4×10^{15} molecules cm^{-3} of cyclohexane being present in the photolysis experiments to scavenge any OH radicals formed.

Nitrate radicals were produced from the thermal decomposition of N_2O_5, and NO_2 was also included in the reactant mixtures. The initial reactant concentrations (molecules cm^{-3}) were as follows: dichlorvos and reference compound, ~2.4×10^{13} each; NO_2, $(4.8-9.6) \times 10^{13}$; ethane $(3.2-4.1) \times 10^{15}$ (to scavenge any Cl atoms generated); and three additions of N_2O_5 (each addition corresponding to $(0.53-1.76) \times 10^{13}$ molecules cm^{-3} of N_2O_5 in the chamber) were made to the chamber during an experiment.

The concentrations of dichlorvos and the reference compounds were measured during the experiments by gas chromatography with flame ionization detection (GC-FID). Kinetic experiments consisted of three irradiation periods or three N_2O_5 additions, and GC-FID analyses were carried out prior to reaction (with replicate analyses) and after each irradiation period or N_2O_5 addition, with a replicate GC-FID analysis after the third (and last) irradiation period or N_2O_5 addition. For the analysis of dichlorvos, methacrolein, thiophene, di-*n*-butyl ether and 1,3,5-trimethylbenzene, gas samples of 100 cm^3 volume were collected from the chamber onto Tenax-TA solid adsorbent, with subsequent thermal desorption at ~205 °C onto a 30 m DB-1701 megabore column held at −40 or 0 °C and then temperature programmed to 200 °C at 8 °C min^{-1}. For the analysis of *trans*-2-butene, gas samples were collected from the chamber into 100 cm^3 volume all-glass gastight syringes and transferred via a 1 cm^3 gas sampling loop onto a 30 m DB-5 megabore column initially held at −25 °C and then temperature programmed to 200 °C at 8 °C min^{-1}. Replicate analyses in the chamber in the dark agreed to within 5% for dichlorvos (typically to within 2−3%) and to within 3% for the reference compounds.

The rate constant for the reaction of dichlorvos with O_3 was determined by monitoring the decay of dichlorvos in the presence of a known concentration of O_3,[8,10] with cyclohexane being present to scavenge any OH radicals formed. Assuming that under these conditions the only loss process for dichlorvos was by reaction with O_3 and wall loss, then,

$$\ln([\text{dichlorvos}]_{t_o}/[\text{dichlorvos}]_t) - k_w(t - t_o) - D_t = k_3[O_3](t - t_o) \qquad (II)$$

where D_t (= 0.0027) is the small amount of dilution caused by the initial addition of O_3 to the chamber, k_w is the wall loss rate and k_3 is the rate constant for reaction 3.

$$O_3 + \text{dichlorvos} \rightarrow \text{products} \qquad (3)$$

The initial reactant concentrations (molecules cm^{-3}) were as follows: dichlorvos, ~2.4×10^{13}; O_3, $(5.98-6.31) \times 10^{13}$; and cyclohexane, 2.4×10^{15}. O_3 concentrations were measured during the 4.9−5.1 h duration reactions by ultraviolet absorption, and the concentrations of dichlorvos were measured by GC-FID as described above.

Products of the OH Radical Reactions. Products of the reaction of OH radicals with dichlorvos were investigated using in situ API-MS spectrometry and in situ FT-IR spectroscopy. No product peaks from reaction of dichlorvos were observed using GC-FID analyses.

Experiments with API-MS Analyses. In these experiments, the chamber contents were sampled through a 25 mm diameter ×75 cm length Pyrex tube at ~20 L min^{-1} directly into the API mass spectrometer source. The operation of the API-MS in the MS (scanning) and MS/MS (with collision activated dissociation) modes has been described previously,[8,10] and both positive and negative ion modes were used in this work. In the positive ion mode, protonated water hydrates ($H_3O^+(H_2O)_n$) generated by the corona discharge in the chamber diluent air were responsible for the protonation of analytes, and the ions that were mass analyzed were mainly protonated molecules ($[M + H]^+$) and their protonated homo- and heterodimers. In the negative ion mode, negative ions are generated by the negative corona around the discharge needle, and under the conditions employed, O_2^-, NO_2^-, and NO_3^- were the major relevant negative ions. Instrument tuning and operation were designed to induce cluster formation. For the OH radical reaction, the initial reactant concentrations (molecules cm^{-3}) were as follows: CH_3ONO and NO, ~2.4×10^{13} each; and dichlorvos, ~1.2×10^{13}; and irradiations were carried out for 3 min, corresponding to ~25% reaction of the initially present dichlorvos. For the NO_3 radical reaction, the reactant concentrations (molecules cm^{-3}) were

as follows: dichlorvos, ~1.2×10^{13}; and NO_2, ~4.8×10^{13}; and one addition of N_2O_5 (corresponding to 6.5×10^{12} molecules cm^{-3} of N_2O_5 in the chamber) was made to the chamber during the experiment.

Experiments with FT-IR Analyses. Dichlorvos, in amounts equivalent to $(1.00-1.09) \times 10^{14}$ molecules cm^{-3} in the chamber, was introduced as vapor into the evacuated chamber, thus minimizing possible decomposition as this procedure required less heating. Dichlorvos was observed to "stick" to the chamber walls, but attained a near-equilibrium vapor concentration after a time period which depended upon wall conditioning. After introducing dichlorvos, the first spectrum in EC-2202 showed only ~12% of the amount introduced to be in the vapor phase (using the solution-phase IR calibration; see below). In the first two experiments (EC-2202 and −2203), 90−120 min were required to attain an equilibrium (or near-equilibrium) dichlorvos concentration of $(4.67-4.96) \times 10^{13}$ molecules cm^{-3}, while in the third experiment (EC-2204) where the chamber had sat idle for several days with an atmosphere of pure N_2 gas, it required >4 h to attain an equilibrium dichlorvos concentration of 3.00×10^{13} molecules cm^{-3}. After these equilibration periods, the dichlorvos concentrations remained constant during additional 30−60 min periods prior to irradiation during which time period diluent air was added to bring the pressure to atmospheric and CH_3ONO and NO were flushed into the chamber.

A gas-phase FT-IR calibration for dichlorvos employing direct introduction of its vapor into the chamber was obviously not possible. Therefore, the quantitative measurement of this compound was based on the integrated band coefficient derived from dilute CCl_4 solutions (8.41×10^{-4} M and 3.36×10^{-3} M) using a 1.09 mm path length NaCl liquid cell. The integrated coefficient of the solution band at 1050 cm^{-1} was measured as 4.79×10^{-17} cm molecule^{-1} which was applied to the corresponding vapor absorption band at 1063 cm^{-1}.

Irradiations of CH_3ONO [or $(CH_3)_2CHONO$)]−NO−dichlorvos−air mixtures were carried out in the 5870 L evacuable chamber, with initial reactant concentrations (molecules cm^{-3}) of : CH_3ONO, 2.46×10^{14}, or $(CH_3)_2CHONO$, 1.45×10^{14}; NO, 2.46×10^{14}; and dichlorvos (amount in gas phase; see above), $(3.00-4.96) \times 10^{13}$. Irradiations were carried out intermittently for 5−8 min intervals, with spectra being recorded during the intervening dark periods. Total irradiation times were 25−37 min, resulting in up to 64−68% consumption of the initial gas-phase dichlorvos. IR spectra were recorded with 32 scans per spectrum (corresponding to a 1.2 min averaging time) at a full-width-at-half-maximum resolution of 0.7 cm^{-1} and a path length of 62.9 m. The quantitative analysis of products and reactants by FT-IR spectroscopy was carried out by a subtractive procedure, in which components were successively subtracted from the spectrum of the mixture using calibrated spectra of the gaseous reactants and known products which have been recorded previously with the same instrument and identical spectral parameters.[8,10,14] As routinely carried out, the absorption bands of CH_3ONO, or $(CH_3)_2CHONO$, and NO and of their photooxidation products (for example, NO_2, HCHO, CH_3ONO_2, HNO_3, and HONO from CH_3ONO) were subtracted first to more clearly reveal the products from the main reactant.

Aerosol Formation. To assess the importance of aerosol formation from the OH radical-initiated reaction of dichlorvos, an irradiation of a CH_3ONO−NO−dichlorvos−air mixture were carried out at 296 ± 2 K in a ~7000 L Teflon chamber, with dichlorvos being monitored by GC-FID as described above and with aerosol number density and size distribution being measured using a TSI 3936L72 scanning mobility particle sizer (SMPS). The initial reactant concentrations were similar to those in the kinetic experiments (see above).

Chemicals. The chemicals used, and their stated purities, were as follows: di-*n*-butyl ether (99+%), methacrolein (95%), thiophene (99+%), and 1,3,5-trimethylbenzene (98%), Aldrich; dichlorvos (99.3%), Sigma-Aldrich; and *trans*-2-butene (≥95%) and NO (≥99.0%), Matheson Gas Products. Methyl nitrite, 2-propyl nitrite and N_2O_5 were prepared and stored as described previously,[8,10] and O_3 in O_2 diluent was generated using a Welsbach T-408 ozone generator. NO_2 was prepared as needed by reacting NO with an excess of O_2.

RESULTS

Photolysis and Dark Decays. In the ~7000-L Teflon chamber at 296 ± 2 K, the gas-phase dichlorvos concentrations decayed in the dark at rates of $(3.9 \pm 2.2) \times 10^{-6}$ s^{-1} over 6.8 h and $(4.1 \pm 1.9) \times 10^{-6}$ s^{-1} over 5.2 h, where (as throughout unless noted otherwise) the indicated errors are two standard deviations. Over periods of 5.0 and 4.9 h which included four 15 min irradiation periods at the same light intensity and spectral distribution as used in the room temperature OH radical rate constant determinations, the measured dichlorvos concentrations decayed at rates of $(3.6 \pm 4.6) \times 10^{-6}$ s^{-1} and $(4.0 \pm 6.8) \times 10^{-6}$ s^{-1}, respectively. There was therefore no evidence for photolysis of dichlorvos over the time periods used in the OH radical kinetic experiments, nor for desorption of dichorvos from the chamber walls due to slight heating of the chamber walls during the irradiation periods (as has been observed previously for phthalide and 1,2-diacetylbenzene[20]). Measured dichlorvos concentrations for experiments conducted in this chamber were therefore corrected for wall loss using a decay rate of 4.0×10^{-6} s^{-1} (1.44% h^{-1}).

In the ~5000-L Teflon bag used for temperature-dependent experiments, dichlorvos decay rates of $(5.9 \pm 1.8) \times 10^{-6}$ s^{-1} (2.1 ± 0.7% h^{-1}) over 4.7 h at 298 K and $(3.2. \pm 1.3) \times 10^{-6}$ s^{-1} (1.1 ± 0.5% h^{-1}) over 4.7 h at 346 K were determined and used to correct the measured dichlorvos concentrations in this chamber for wall decay at 299 ± 2 K and 348 ± 2 K, respectively. An average value of the wall decay of 4.5×10^{-6} s^{-1} (1.6% h^{-1}) was used to correct the dichlorvos data for the experiments at 322 ± 2 K.

Rate Constant for Reaction with O_3. In the presence of average O_3 concentrations of $(5.42-5.71) \times 10^{13}$ molecules cm^{-3} and with 2.4×10^{15} molecules cm^{-3} of cyclohexane present to scavenge any OH radicals formed, a 4−15% increase in the measured dichlorvos concentration was observed within 6 min after addition of O_3, followed by a slow decrease in the measured dichlorvos concentration with reaction time. While the O_3 concentrations decreased during the reactions at a rate of ~4% h^{-1}, a factor of ~2 higher than the background O_3 decay rate in pure air in this chamber, the O_3 concentrations throughout an experiment were within ±10% of the average value. Since the average O_3 concentrations in the three experiments were identical to within 5%, the dichlorvos data from all three experiments are plotted in accordance with eq II in Figure 1. A least-squares analysis of the entire data set (omitting the 0,0 point defined by the prereaction analyses) leads to $k_3(O_3 + \text{dichlorvos}) = (1.7 \pm 0.5) \times 10^{-19}$ cm^3 $molecule^{-1}$ s^{-1} at 296 ± 2 K. Taking into account

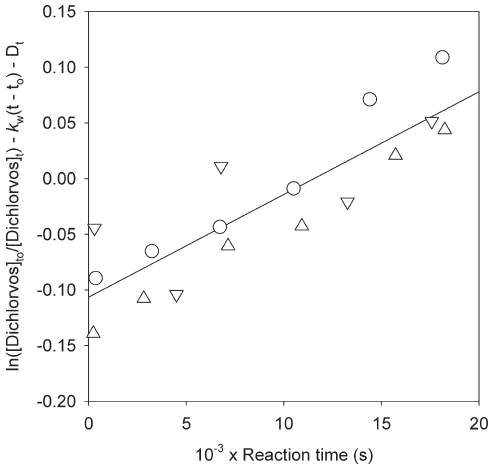

Figure 1. Plot of eq II for the reaction of O_3 with dichlorvos at 296 ± 2 K. Cyclohexane was present to scavenge any OH radical formed (see text). The differing symbols denote the 3 experiments conducted (see text).

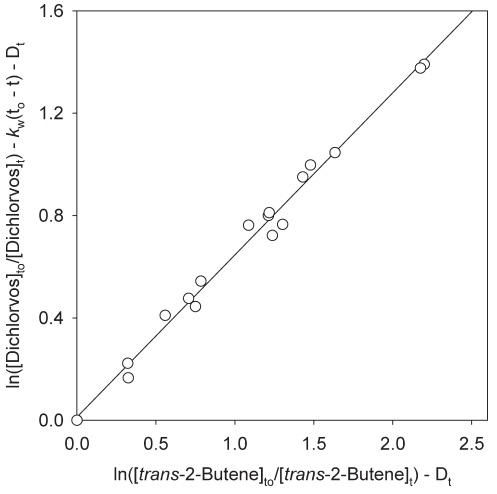

Figure 2. Plot of eq I for the reaction of NO_3 radicals with dichlorvos at 296 ± 2 K, with *trans*-2-butene as the reference compound. Ethane was present in all 4 experiments to scavenge any Cl atoms formed (see text).

additional uncertainties caused by the behavior of the dichlorvos and the small amounts reacted during these experiments (Figure 1), we cite the rate constant for the O_3 reaction to be

$$k_3(O_3 + \text{dichlorvos}) = (1.7 \pm 1.0) \times 10^{-19}$$
$$\text{cm}^3\ \text{molecule}^{-1}\ \text{s}^{-1} \text{ at } 296 \pm 2\text{K}$$

Rate Constant for Reaction with NO_3 Radicals. Initial experiments at 296 ± 2 K with methacrolein and thiophene as the reference compounds showed that dichlorvos was significantly more reactive than either of these reference compounds. Therefore, *trans*-2-butene was used as the reference compound, and data from reacting N_2O_5−NO_3−NO_2−dichlorvos−*trans*-2-butene−ethane−air mixtures in the ~7000-L Teflon chamber at 296 ± 2 K are plotted in accordance with eq I in Figure 2. Ethane was present in the reactant mixtures to scavenge any Cl atoms formed from the NO_3 + dichlorvos reaction. Least squares analysis of these data leads to a rate constant ratio k_1/k_2 of 0.634 ± 0.035 at 296 ± 2 K.

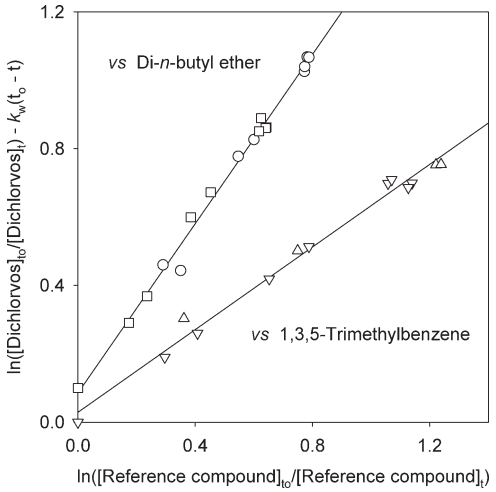

Figure 3. Plots of eq I for the reaction of OH radicals with dichlorvos at 296 ± 2 K, with di-*n*-butyl ether and 1,3,5-trimethylbenzene as the reference compounds. □, ▽, ethane present to scavenge any Cl atoms formed (see text); ○, Δ, no ethane present. The dichlorvos data with di-*n*-butyl ether as the reference compound have been displaced vertically by 0.10 units for clarity.

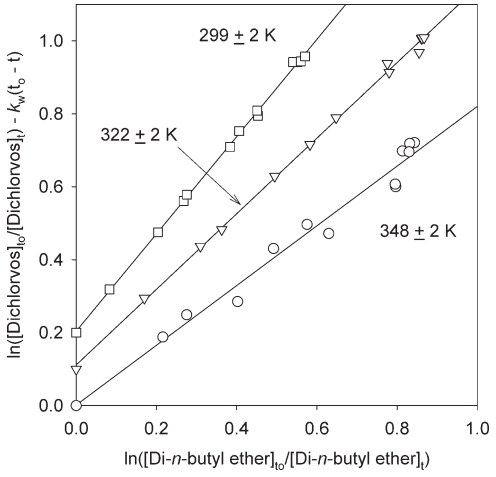

Figure 4. Plots of eq I for the reaction of OH radicals with dichlorvos at 299 ± 2, 322 ± 2, and 348 ± 2 K, with di-*n*-butyl ether as the reference compounds. Data are from 3 experiments at each temperature, and ethane was not present in the reactant mixtures. The dichlorvos data at 322 ± 2 and 299 ± 2 K have been displaced vertically by 0.10 and 0.20 units, respectively, for clarity.

This rate constant ratio is placed on an absolute basis by use of a rate constant for the reaction of NO_3 radicals with *trans*-2-butene of $k_2 = 3.89 \times 10^{-13}$ at 296 K,[1] resulting in the following:

$$k_1(NO_3 + \text{dichlorvos}) = (2.47 \pm 0.14) \times 10^{-13}$$
$$\text{cm}^3\ \text{molecule}^{-1}\ \text{s}^{-1} \text{ at } 296 \pm 2\text{K}$$

Taking into account the estimated overall uncertainties in the rate constant k_1 due to reactant measurement uncertainties, wall loss rates, and in the rate constant for the reference compound results in a rate constant of the following:

$$k_1(NO_3 + \text{dichlorvos}) = (2.5 \pm 0.5) \times 10^{-13}$$
$$\text{cm}^3\ \text{molecule}^{-1}\ \text{s}^{-1} \text{ at } 296 \pm 2\text{K}$$

dx.doi.org/10.1021/jp112019s |J. Phys. Chem. A 2011, 115, 2756–2764

Table 1. Rate Constant Ratios k_1/k_2 and Rate Constants k_1 for the Reaction of OH Radicals with Dichlorvos

temperature (K)	reference compound	k_1/k_2[a]	$10^{11} \times k_1$ (cm^3 $molecule^{-1}$ s^{-1})[b]
296 ± 2[c]	1,3,5-trimethylbenzene	0.604 ± 0.040	3.42 ± 0.23
296 ± 2[c]	di-*n*-butyl ether	1.24 ± 0.06	3.49 ± 0.17
299 ± 2[d]	di-*n*-butyl ether	1.33 ± 0.03	3.67 ± 0.09
322 ± 2[d]	di-*n*-butyl ether	1.04 ± 0.03	2.52 ± 0.08
348 ± 2[d]	di-*n*-butyl ether	0.819 ± 0.075	1.77 ± 0.17

[a] Indicated errors are two least-squares standard deviations. [b] Placed on an absolute basis by use of rate constants k_2 for the reaction of OH radicals with 1,3,5-trimethylbenzene and di-*n*-butyl ether of 5.67×10^{-11} cm^3 $molecule^{-1}$ s^{-1} at 296 K[1] and 6.29×10^{-18} T^2 $e^{1164/T}$ cm^3 $molecule^{-1}$ s^{-1},[21] respectively. Indicated errors are two least-squares standard deviations and do not include uncertainties associated with the rate constants k_2, which are estimated to be ~±10%. [c] Carried out in a ~7000 L Teflon chamber. Measured dichlorvos concentrations corrected for wall loss using a decay rate of 4.0×10^{-6} s^{-1} (see text). [d] Carried out in a ~5000 L Teflon bag. Measured dichlorvos concentrations corrected for wall loss using decay rates of 5.9×10^{-6} s^{-1} at 299 ± 2 K, 4.5×10^{-6} s^{-1} at 322 ± 2 K and 3.2×10^{-6} s^{-1} at 348 ± 2 K (see text).

Rate Constants for Reaction with OH Radicals. The data obtained from irradiations of $CH_3ONO-NO-$dichlorvos$-$di-*n*-butyl ether$-$air and $CH_3ONO-NO-$dichlorvos$-$1,3,5-trimethylbenzene$-$air mixtures are plotted in accordance with eq I in Figures 3 and 4. The rate constant ratios k_1/k_2 and rate constants k_1 obtained by least-squares analyses of the experimental data are given in Table 1. Ethane was present in a number of the experiments carried out at 296 ± 2 K in the ~7000-L Teflon chamber to scavenge any Cl atoms formed, and the data in the presence or absence of ethane were indistinguishable within the experimental uncertainties (Figure 3).

The rate constants listed in Table 1 are plotted in Arrhenius form in Figure 5, and the Arrhenius expression obtained from least-squares analyses of our data is as follows:

$$k_1(\mathrm{OH} + \mathrm{dichlorvos}) = 3.53 \times 10^{-13} e^{(1367 \pm 239)/T}$$

$$cm^3\ molecule^{-1}\ s^{-1}$$

with a 298 K rate constant of $k_1(\mathrm{OH} + \mathrm{dichlorvos}) = 3.47 \times 10^{-11}$ cm^3 $molecule^{-1}$ s^{-1}. Taking into account the estimated overall uncertainties in the rate constant ratios, then,

$$k_1(\mathrm{OH} + \mathrm{dichlorvos}) = (3.5 \pm 0.7) \times 10^{-11}$$

$$cm^3\ molecule^{-1}\ s^{-1}\ \text{at}\ 298 \pm 2K$$

with an estimated overall uncertainty in the value of B in $k = A\,e^{-B/T}$ of ±400 K.

Products of the OH and NO_3 Radical-Initiated Reactions. *Analyses by in Situ FT-IR.* Irradiations of two $CH_3ONO-NO-$dichlorvos$-$air mixtures and one $(CH_3)_2CHONO-NO-$dichlorvos$-$air mixture were carried out, and the results are given in Table 2. The major products observed were phosgene [$C(O)Cl_2$], dimethyl phosphate [$(CH_3O)_2P(O)OH$] and CO measured at their respective band positions at 857 (and also 1832), 1071 and 2143 cm^{-1}, as shown in Figure 6 for $C(O)Cl_2$ and $(CH_3O)_2P(O)OH$. The CO yield could only be measured from the irradiation employing 2-propyl nitrite as the OH radical precursor, because photooxidation of CH_3ONO yields HCHO which reacts with OH radicals to form CO in significant amounts. Corrections to the measured CO yields to take into account CO formation from photooxidation of 2-propyl nitrite were negligible.[8,10]

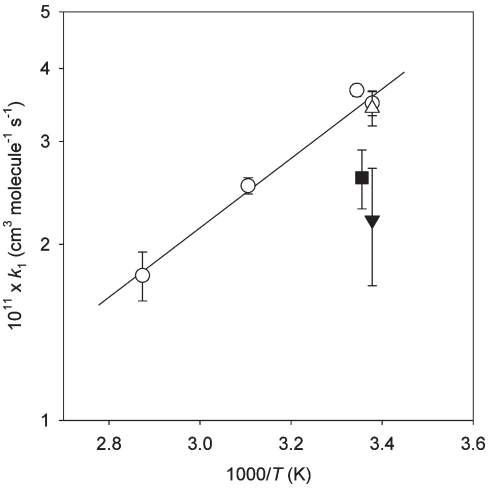

Figure 5. Arrhenius plot of the rate constant k_1 for the reaction of OH radicals with dichlorvos. ○, This work, relative to di-*n*-butyl ether from experiments in ~5000 or ~7000 L Teflon chambers; Δ, this work, relative to 1,3,5-trimethylbenzene from experiments in a ~7000 L Teflon chamber; ▼, Sun et al.;[9] ■, Feigenbrugel et al.[11] The error bars associated with the rate constants measured here (○, Δ) are two standard deviations.

Phosgene yields from the two irradiated dichlorvos$-CH_3O-NO-NO-$air mixtures were quite similar, being in the range 67−81%, with those from the dichlorvos$-(CH_3)_2CHONO-NO-$air mixture being slightly higher at 85−92% (Table 2). These yield ranges that are within the experimental uncertainties, considering the potential variability of desorption of dichlorvos from the walls in these experiments. While the data in Table 2 suggest a slight increase in the $C(O)Cl_2$ yield with increasing extent of reaction during each experiment, least-squares analyses show that the intercepts of plots of ([$C(O)Cl_2$] formed) against ([dichlorvos] reacted) are within 1.1 standard deviations of zero, indicating no statistically significant increase in $C(O)Cl_2$ yield with increasing extent of reaction. Least-squares analyses of the combined data result in a $C(O)Cl_2$ formation yield of 76 ± 8% and a CO yield within 10% of that for $C(O)Cl_2$, with CO yield = (1.04 ± 0.06) × $C(O)Cl_2$ yield. The $(CH_3O)_2P(O)OH$ yields decreased with irradiation time in all experiments (Table 2), as expected from previous work in this chamber which showed that $(CH_3O)_2P(O)OH$ decays to the walls.[7] Extrapolation to zero irradiation time (or zero extent of reaction) indicates a $(CH_3O)_2P(O)OH$ yield ≥0.60 of the $C(O)Cl_2$ yield.

The spectrum of dichlorvos at its initial equilibrium concentration in the chamber and the product spectrum after 25 min irradiation of the $CH_3ONO-NO-$dichlorvos$-$air mixture in experiment EC-2203 are shown in Figure 6. In addition to the major products $C(O)Cl_2$, $(CH_3O)_2P(O)OH$, and CO (the latter not evident in Figure 6 because it absorbs outside of the frequency range shown), two unidentified products with relatively small yields were indicated by weak absorption bands at 1799 cm^{-1} and 1675 cm^{-1} in the product spectrum (Figure 6),

Table 2. Results of OH + Dichlorvos Experiments Utilizing in Situ FT-IR Spectroscopy for Analysis (See Also Text)

		concentration (in units of 10^{13} molecules cm^{-3})[a]					
experiment number	irradiation time (min)	Δdichlorvos	$C(O)Cl_2$	$(CH_3O)_2P(O)OH$	CO	>C═O estimate	$RONO_2$ estimate
EC-2202[b]	5	1.25	0.86 (69%)	0.66 (53%)			
	10	1.99	1.45 (73%)	0.89 (44%)			
	15	2.29	1.80 (78%)	0.64 (28%)			
	20	2.71	2.16 (80%)	0.69 (25%)			
	25	2.98	2.41 (81%)	0.64 (21%)			
EC-2203[b]	5	1.43	0.96 (67%)	0.79 (55%)		0.10 (7%)	0.07 (5%)
	10	2.16	1.55 (72%)	0.86 (40%)		0.25 (12%)	0.10 (5%)
	15	2.76	2.04 (74%)	0.84 (30%)		0.39 (14%)	0.17 (6%)
	20	3.10	2.34 (75%)	0.79 (25%)		0.62 (20%)	0.30 (10%)
	25	3.35	2.55 (77%)	0.69 (21%)		0.89 (27%)	0.32 (10%)
EC-2204[c]	5	0.66	0.57 (85%)	0.37 (56%)	0.52 (78%)		
	13	1.18	1.01 (89%)	0.42 (37%)	0.96 (85%)		
	21	1.45	1.33 (92%)	0.42 (29%)	1.35 (93%)		
	29	1.77	1.60 (90%)	0.42 (24%)	1.67 (94%)		
	37	1.99	1.80 (90%)	0.42 (21%)	1.82 (91%)		

[a] Values in parentheses are the calculated molar yields. [b] Irradiations of $CH_3ONO-NO-$dichlorvos$-$air mixture, with an initial gas-phase dichlorvos concentrations of 4.67×10^{13} molecules cm^{-3} (EC-2202) and 4.96×10^{13} molecules cm^{-3} (EC-2203). [c] Irradiation of a $(CH_3)_2CHONO-NO-$dichlorvos$-$air mixture, with an initial gas-phase dichlorvos concentration of 3.00×10^{13} molecules cm^{-3}.

corresponding to a carbonyl compound and, possibly, an organic nitrate ($RONO_2$), respectively. The 1675 cm^{-1} band was well-isolated, such that the $RONO_2$ formation yield was readily estimated from the band area and the average integrated absorption coefficients of common organic nitrates.[22] An $RONO_2$ yield increasing from ~5% initially to ~10% at the end of the reaction was calculated for EC-2203. The 1799 cm^{-1} band sat on the side of the P-branch of the fundamental band of $C(O)Cl_2$ centered at 1827 cm^{-1}, but did not interfere with measurements of $C(O)Cl_2$ based on the R-branch peak at 1832 cm^{-1} and another stronger peak at 857 cm^{-1}. The contour and area of the 1799 cm^{-1} band were easily approximated, and based on the average absorption coefficient of corresponding bands of other carbonyl compounds,[22] a yield of ~7% initially, increasing to ~27% at the end of the reaction, was calculated for this unknown carbonyl product in EC-2203 (Table 2). The increase in yield with extent of reaction indicates that this carbonyl product is formed mainly as a second-generation product.

Glyoxyloxyl chloride, ClC(O)CHO, a potential product of the OH + dichlorvos reaction (see below), has been isolated by Czarnowski[23] who also recorded its absorption spectrum. The strongest absorption bands of ClC(O)CHO at 781 cm^{-1} and 1777 cm^{-1} [23] are completely absent in the product spectrum presented in Figure 6, and HCl, which can be formed from the hydrolysis of ClC(O)CHO,[23] was also not observed.

API-MS Analyses. Reactions of dichlorvos with OH radicals and NO_3 radicals were carried out with analyses by in situ API-MS and API-MS/MS. In contrast to the case for alkyl phosphates and phosphonates,[8,10,16] ions were observed in both positive and negative ion mode prior to reaction. Since Cl has two major isomers of masses 35 (75%) and 37 (25%), then dichlorvos $[(CH_3O)_2P(O)OCH{=}CCl_2]$ exists as isomers of molecular weight 220, 222, and 224, and the presence of this isomer pattern was evident in both the positive ion and negative ion API-MS spectra prior to reaction (see, for example, Figures 7 and 8).

The API-MS spectra of the OH radical- and NO_3 radical-initiated reactions of dichlorvos show that many of the same mass ion peaks are present from each reaction. Furthermore, in negative ion mode, many of the reaction product peaks (Figures 7 and 8) do not show the triplet structure characteristic of the $=CCl_2$ group, indicating that the reaction product(s) do not contain this group. In positive ion mode, very weak postreaction ion peaks are attributed as follows: 127 u, $[126 + H]^+$ (NO_3 radical reaction only); 473/475/477 u, $[220/222/224 + 126 + 126 + H]^+$; and 505 u, $[126 + 126 + 126 + 126 + H]^+$. The negative ion mode spectra of the OH radical- and NO_3 radical-initiated reactions are shown in Figures 7 and 8, respectively, and the peak attribution from API-MS/MS product ion spectra are given in the captions to these figures. The molecular weight 126 product of the OH radical reaction is attributed to $(CH_3O)_2P(O)OH$, which was identified and quantified in our in situ FT-IR analyses as the major P-containing product. A product of molecular weight 126, presumably $(CH_3O)_2P(O)OH$, is also formed from the NO_3 radical reaction.

Aerosol Formation. Aerosol formation was measured during a $CH_3ONO-NO-$dichlorvos$-$air irradiation in a ~7000 L Teflon chamber at 296 ± 2 K. The initial reactant concentrations and experimental procedures were as in the kinetic experiments, and 63% of the initially present dichlorvos had been consumed by the end of the experiment. The aerosol loading prior to beginning the irradiations and with all of the reactants present in the chamber was 32 $\mu g\ m^{-3}$ (corresponding to 0.4% of the dichlorvos present). No new particle formation was observed during the three irradiation periods; rather the particle size increased as the reaction proceeded. The aerosol yield (defined as aerosol formed/dichlorvos reacted) was independent of the extent of the reaction, and assuming that the aerosol had the same density as dichlorvos, then the aerosol yield was ~1%. This lack of significant aerosol formation is consistent with the in situ FT-IR analyses showing that the gas-phase products CO,

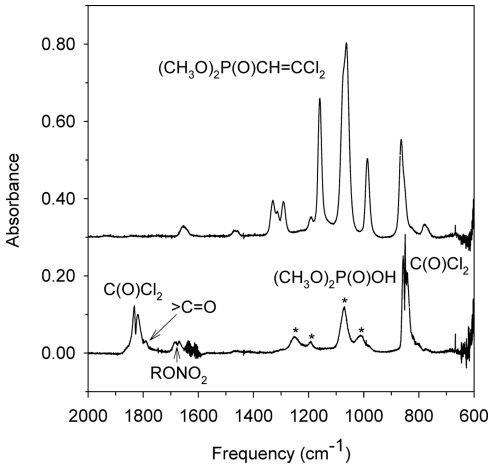

Figure 6. Infrared spectra from experiment EC-2203. Top: initial dichlorvos; Bottom: products of the $CH_3ONO-NO-$dichlorvos$-$air mixture after 25 min of irradiation, after subtraction of IR absorption bands of unreacted dichlorvos and of CH_3ONO and NO and their photooxidation products (see text). The asterisks denote the IR absorption bands of $(CH_3O)_2P(O)OH$.[7] See Table 2 for the concentrations of dichlorvos, $C(O)Cl_2$, $(CH_3O)_2P(O)OH$, $RONO_2$, and the carbonyl product.

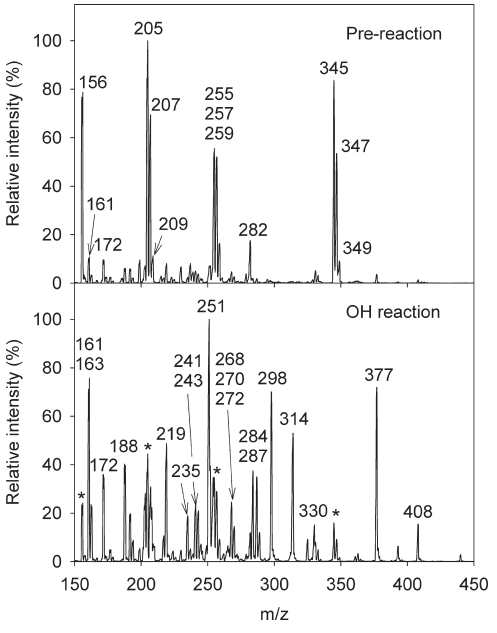

Figure 7. Negative ion mode API-MS spectra of a $CH_3ONO-NO-$dichlorvos$-$air mixture prior to and after irradiation. The labeled peaks in the postreaction spectrum (bottom) are the major ion peaks which were present after reaction but not before, and peaks labeled with an asterisk (*) were present prior to reaction (as shown in the top spectrum). The ion peaks present as a result of reaction are attributed to: 161, $[126 + {}^{35}Cl]^-$; 163, $[126 + {}^{37}Cl]^-$; 172 $[126 + NO_2]^-$; 188 $[126 + NO_3]^-$; 251 $[126 + 126 - H]^-$; 284 $[126 + 126 + O_2]^-$; 298 $[126 + 126 + NO_2]^-$; 314 $[126 + 126 + NO_3]^-$; and 377 $[126 + 126 + 126 - H]^-$. The ion peaks at 241 and 243 u and at 268, 270, and 272 u, which were present in low relative intensity prior to reaction, could arise from adducts of a product of molecular weight 206, 208, and 210 (i.e., containing two Cl atoms) with Cl^- and NO_3^- ions.

$C(O)Cl_2$, and $(CH_3O)_2P(O)OH$ account for the majority of the dichlorvos reacted.

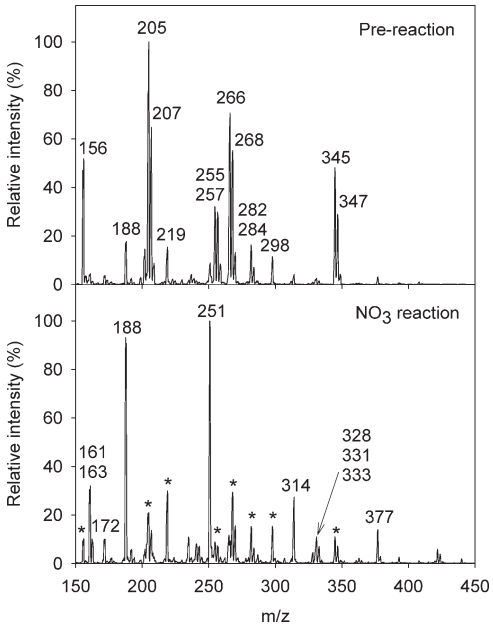

Figure 8. Negative ion mode API-MS spectra of a $N_2O_5-NO_2-$dichlorvos$-$air mixture prior to and after reaction. The labeled peaks in the postreaction spectrum (bottom) are the major ion peaks which were present after reaction but not before, and peaks labeled with an asterisk (*) were present prior to reaction (as shown in the top spectrum). The ion peaks present as a result of reaction are attributed to the following: 161, $[126 + {}^{35}Cl]^-$; 163, $[126 + {}^{37}Cl]^-$; 172 $[126 + NO_2]^-$; 188 $[126 + NO_3]^-$; 251 $[126 + 126 - H]^-$; 314 $[126 + 126 + NO_3]^-$; and 377 $[126 + 126 + 126 - H]^-$. While the ion peaks in the postreaction spectrum at 328, 331, and 333 u were present at low relative intensity prior to reaction, they may also be associated with a reaction product(s).

DISCUSSION

These are, to our knowledge, the first reported rate constants for the reactions of dichlorvos with NO_3 radicals and O_3. The presence of the $-CH{=}CCl_2$ moiety enhances the reactivity toward O_3 and, especially, NO_3 radicals, with the rate constants for the reactions of O_3 and NO_3 radicals with dichlorvos being factors of >2.5 and ≥500, respectively, higher than those previously measured for a series of alkyl phosphates and phosphonates.[8,10,16]

Our room temperature rate constant for the reaction of dichlorvos with OH radicals of $(3.5 \pm 0.7) \times 10^{-11}$ cm^3 $molecule^{-1}$ s^{-1} at 298 K can be compared to the previously reported values of Sun et al.,[9] of $(2.2 \pm 0.5) \times 10^{-11}$ cm^3 $molecule^{-1}$ s^{-1} at 296 ± 1 K relative to styrene [after re-evaluation using the recommended rate constant for OH + styrene[1]] and Feigenbrugel et al.,[11] of $(2.6 \pm 0.3) \times 10^{-11}$ cm^3 $molecule^{-1}$ s^{-1} at 298 ± 5 K relative to 1,3,5-trimethylbenzene and cyclohexane (see also Figure 5). Both Sun et al.[9] and Feigenbrugel et al.[11] reported wall and/or photolysis losses of dichlorvos, at rates of $(2.17 \pm 0.33) \times 10^{-4}$ s^{-1} in a 28.5 L quartz reactor[9] and $(9.3 \pm 0.3) \times 10^{-6}$ s^{-1} in the ~204 000 L EUPHORE chamber[11] and took these into account in their data analysis (wall losses accounted for ≥30% and ~15% of the measured dichlorvos disappearance rates in the Sun et al.[9] and Feigenbrugel et al.[11] studies, respectively). Feigenbrugel et al.[11] observed no evidence for photolysis ($k_{phot} < 5 \times 10^{-6}$ s^{-1}) for summertime sunlight irradiation at 39.5° latitude. Surprisingly, the measured dichlorvos decay rate in the ~204000 L EUPHORE chamber[11] was

Scheme 1.[a]

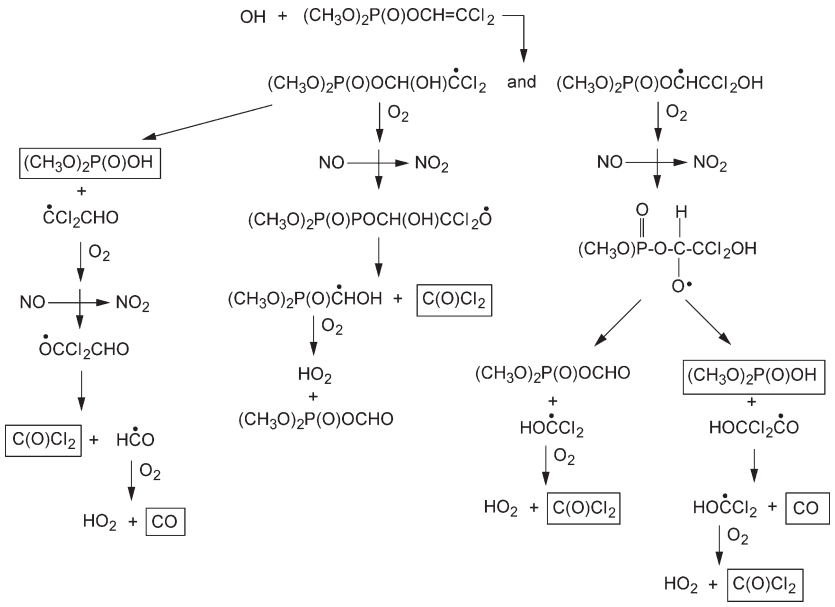

[a] Observed products are shown in boxes. Possible decomposition of the $^{\bullet}OCCl_2CHO$ radical to Cl + ClC(O)CHO is not shown (see text).

higher than observed in the present study in a ~7000 L chamber. While our 298 K rate constant is a factor of 1.35 higher than that of Feigenbrugel et al.,[11] the rate constants are in agreement within their cited uncertainties.

Wall adsorption and/or desorption of dichlorvos was clearly occurring in our 5870 L evacuable chamber, which has numerous "O" rings to connect flanges and window assemblies to the chamber body. In contrast to the our previous studies of alkyl phosphates and phosphonates in this chamber,[8,10,16] where an initial rapid decrease in the organophosphorus compound concentration was followed by a slower decay rate,[8] in the present experiments dichlorvos appeared to initially partition mainly to the chamber walls and/or fittings followed by a slow desorption back into the gas phase. Although the FT-IR data showed no evidence for desorption from the walls during the actual reaction periods, the measured product yields, defined as ([product] formed)/([dichlorvos] reacted), are clearly subject to significant uncertainties and may be upper limits because of desorption of dichlorvos from the chamber walls as the reactions proceeded. However, on a relative basis, the formation yields of CO and $C(O)Cl_2$ and, to a lesser extent because of its wall decay, of $(CH_3O)_2P(O)OH$ from the OH radical-initiated reaction are well-defined.

Our FT-IR analyses, supported by the API-MS analyses, show that the major products of the OH radical-initiated reaction of dichlorvos are CO, $C(O)Cl_2$ and $(CH_3O)_2P(O)OH$, with CO and $C(O)Cl_2$ being formed in equal yield (to within 10%) and with measured $C(O)Cl_2$ and $(CH_3O)_2P(O)OH$ yields of 76 ± 8% and ≥45% (initial), respectively, where the error is two standard deviations of least-squares analysis of the data presented in Table 2. Feigenbrugel et al.[11] also observed formation of CO and $C(O)Cl_2$, with the CO yields increasing with the extent of reaction and differing significantly in the two experiments conducted. Feigenbrugel et al.[11] reported molar $C(O)Cl_2$ yields of 66 ± 5% and 47 ± 3% for their two experiments and molar CO yields of 20−73% during one experiment and 43−149% during the second experiment. Considering the uncertainties in both studies, the two studies are in general agreement, although there are obvious differences concerning the effect of extent of reaction on the CO yield. In our experiments 64−68% of the initial gas-phase dichlorvos was consumed by the end of the experiments, whereas in the Feigenbrugel et al.[11] study essentially complete consumption of dichlorvos occurred and the CO yield increased rapidly toward the end of their reactions.[11]

For the OH radical-initiated reactions, there are two likely reaction pathways, involving H-atom abstraction from the CH_3O groups and OH radical addition to the C=C bond, and these and other reaction pathways have been investigated theoretically by Zhang et al.[19] The H-atom abstraction pathway is expected to ultimately form, at least in part, CO + $CH_3OP(O)(OH)$-$OCH{=}CCl_2$ and/or $CH_3OP(O)(OCHO)OCH{=}CCl_2$.[10,19] OH radical addition to the $-CH{=}CCl_2$ moiety can occur at either of the two carbon atoms of the >C=C< bond, as shown in Scheme 1, and Zhang et al.[19] calculate that OH radical addition at the internal carbon, to form $(CH_3O)_2P(O)OCH(OH)C^{\bullet}Cl_2$, is thermochemically favored.

Scheme 1 shows possible reaction pathways after initial OH radical addition to the >C=C< bond, based on previously proposed reaction schemes for other organophosphorus compounds[8,10] and the theoretical calculations of Zhang et al.[19] for OH + dichlorvos, including decomposition of the $(CH_3O)_2$-$P(O)OCH(OH)C^{\bullet}Cl_2$, radical to $(CH_3O)_2P(O)OH$ + $^{\bullet}CCl_2$-CHO.[19] Subsequent reaction of the $^{\bullet}CCl_2CHO$ radical will lead to formation of the $^{\bullet}OCCl_2CHO$ radical, which can decompose to $C(O)Cl_2$ + $HC^{\bullet}O$ and/or to Cl + ClC(O)CHO,[24] with decomposition to $C(O)Cl_2$ + $HC^{\bullet}O$ being more thermochemically favorable than to Cl + ClC(O)CHO by ~6 kcal mol^{-1}.[25,26]

If OH addition to the internal carbon dominates, forming the $(CH_3O)_2P(O)OCH(OH)C^{\bullet}Cl_2$ radical, then unless $(CH_3O)_2$-$P(O)OCHO$ is rapidly and essentially quantitatively transformed into CO + $(CH_3O)_2P(O)OH$ by reaction or elimination of CO, the only presently proposed pathway leading to CO + $C(O)Cl_2$ + $(CH_3O)_2P(O)OH$ is via the $(CH_3O)_2P(O)OCH(OH)C^{\bullet}Cl_2$ radical decomposition pathway identified by Zhang et al.[19] If

this pathway is operative, then the intermediate $^{\bullet}OCCl_2CHO$ radical must decompose to $C(O)Cl_2 + HC^{\bullet}O$ (as shown in Scheme 1) since we did not observe formation of ClC(O)CHO and there was no evidence for involvement of Cl atoms (see Figure 3). Similarly, if OH radical addition to the terminal carbon dominates, forming the $(CH_3O)_2P(O)OC^{\bullet}HCl_2OH$ radical, then the only obvious pathway leading to $CO + C(O)Cl_2 + (CH_3O)_2P(O)OH$ is via the previously proposed[8] rearrangement of the $(CH_3O)_2P(O)OCH(O^{\bullet})CCl_2OH$ radical via a 5-member ring transition state (Scheme 1). Other reaction pathways subsequent to the initial OH radical addition are expected to lead to $C(O)Cl_2 + (CH_3O)_2P(O)OCHO$, with $(CH_3O)_2P(O)OCHO$ possibly reacting with water to form $(CH_3O)_2P(O)OH + HC(O)OH$ or eliminating CO. Only if $(CH_3O)_2P(O)OCHO$ rapidly eliminates CO to form $CO + (CH_3O)_2P(O)OH$ would these pathways be consistent with our product data. The room temperature rate constant for OH + dichlorvos is a factor of ~5 higher than that for OH + trimethyl phosphate $[(CH_3O)_3PO]$,[3] consistent with our conclusion that the major reaction pathway for OH + dichlorvos involves OH radical addition to the >C═C< bond to form $CO + C(O)Cl_2 + (CH_3O)_2P(O)OH$.

Our observation that the rate constant for the reaction of NO_3 radicals with dichlorvos is approximately 3 orders of magnitude higher than those for the alkyl phosphates and alkyl phosphonates previously studied[8,10,16] suggests that the NO_3 radical reaction proceeds by initial addition of NO_3 to the >C═C< bond. Our API-MS analyses also suggest that $(CH_3O)_2P(O)OH$ is a product of this reaction, and a plausible reaction scheme is one analogous to the OH radical reaction shown in Scheme 1, with the NO_3 radical adding to the terminal carbon to form the $(CH_3O)_2P(O)OC^{\bullet}HCl_2ONO_2$ radical. Rearrangement of the subsequently formed $(CH_3O)_2P(O)OCH(O^{\bullet})CCl_2ONO_2$ alkoxy radical via a 5-member transition state would result in formation of $(CH_3O)_2P(O)OH + O_2NOCCl_2C^{\bullet}O$, with the latter decomposing to form $CO + C(O)Cl_2 + NO_2$.

ATMOSPHERIC IMPLICATIONS

The lifetimes of gaseous dichlorvos with respect to reactions with OH radicals, NO_3 radicals, and O_3 can be calculated by combining our measured rate constants with assumed ambient atmospheric concentrations of: OH, an average 12-h daytime concentration of 2×10^6 molecules cm^{-3}; NO_3, a 12-h nighttime concentration of 5×10^8 molecules cm^{-3}; and O_3, a 24-h average concentration of 7×10^{11} molecules cm^{-3} (30 parts-per-billion). The calculated dichlorvos lifetimes of 4 h for reaction with OH radicals during daytime, 2 h for reaction with NO_3 during nighttime and 10 days for reaction with O_3, together with a photolysis lifetime of >4.6 days,[11] indicates that daytime reaction with OH radicals and nighttime reaction with NO_3 radicals will be the dominant dichlorvos chemical loss processes in the atmosphere. Gaseous dichlorvos will therefore be transformed in the atmosphere within typically a few hours, leading to the formation of phosgene $[C(O)Cl_2]$ and dimethyl phosphate $[(CH_3O)_2P(O)OH]$ as major products and with little aerosol formation.

AUTHOR INFORMATION

Corresponding Author

* Tel: (951) 827-4191. E-mail: ratkins@mail.ucr.edu.

ACKNOWLEDGMENT

This work was supported by ENSCO, Inc. While this research has been funded by this agency, the results and content of this publication do not necessarily reflect the views and opinions of the funding agency. R.A. thanks the University of California Agricultural Experiment Station for partial salary support.

REFERENCES

(1) Atkinson, R.; Arey, J. *Chem. Rev.* **2003**, *103*, 4605.
(2) *The Pesticide Manual*, 9th ed., Worthing, C. R., Hance, R. J., Eds.; British Crop Protection Council: Farnham, UK, 1991.
(3) Tuazon, E. C.; Atkinson, R.; Aschmann, S. M.; Arey, J.; Winer, A. M.; Pitts, J. N., Jr. *Environ. Sci. Technol.* **1986**, *20*, 1043.
(4) Goodman, M. A.; Aschmann, S. M.; Atkinson, R.; Winer, A. M. *Arch. Environ. Contam. Toxicol.* **1988**, *17*, 281.
(5) Goodman, M. A.; Aschmann, S. M.; Atkinson, R.; Winer, A. M. *Environ. Sci. Technol.* **1988**, *22*, 578.
(6) Atkinson, R.; Aschmann, S. M.; Goodman, M. A.; Winer, A. M. *Int. J. Chem. Kinet.* **1988**, *20*, 273.
(7) Martin, P.; Tuazon, E. C.; Atkinson, R.; Maughan, A. D. *J. Phys. Chem. A* **2002**, *106*, 1542.
(8) Aschmann, S. M.; Tuazon, E. C.; Atkinson, R. *J. Phys. Chem. A* **2005**, *109*, 2282.
(9) Sun, F.; Zhu, T.; Shang, J.; Han, L. *Int. J. Chem. Kinet.* **2005**, *37*, 755.
(10) Aschmann, S. M.; Tuazon, E. C.; Atkinson, R. *J. Phys. Chem. A* **2005**, *109*, 11828.
(11) Feigenbrugel, V.; Le Person, A.; Le Calvé, S.; Mellouki, A.; Muñoz, A.; Wirtz, K. *Environ. Sci. Technol.* **2006**, *40*, 850.
(12) Aschmann, S. M.; Long, W. D.; Atkinson, R. *J. Phys. Chem. A* **2006**, *110*, 7393.
(13) Aschmann, S. M.; Atkinson, R. *J. Phys. Chem. A* **2006**, *110*, 13029.
(14) Tuazon, E. C.; Aschmann, S. M.; Atkinson, R. *J. Phys. Chem. A* **2007**, *111*, 916.
(15) Aschmann, S. M.; Long, W. D.; Atkinson, R. *J. Phys. Chem. A* **2008**, *112*, 4793.
(16) Aschmann, S. M.; Tuazon, E. C.; Long, W. D.; Atkinson, R. *J. Phys. Chem. A* **2010**, *114*, 3523.
(17) *Handbook of Environmental Fate and Exposure Data for Organic Chemicals, Vol.III: Pesticides*: Howard, P. H., Ed.; Lewis Publishers: Chelsea, MI, 1991.
(18) Agency for Toxic Substances and Disease Registry, Toxic Substances Portal, Dichlorvos, 4. Production, Import, Use, and Disposal, http://www.atsdr.cdc.gov/ToxProfiles/tp88-c4.pdf (accessed February 2011).
(19) Zhang, Q.; Qu, X.; Wang, W. *Environ. Sci. Technol.* **2007**, *41*, 6109.
(20) Wang, L.; Arey, J.; Atkinson, R. *Environ. Sci. Technol.* **2006**, *40*, 5465.
(21) Mellouki, A.; Teton, S.; Le Bras, G. *Int. J. Chem. Kinet.* **1995**, *27*, 791.
(22) Tuazon, E. C.; Atkinson, R. *Int. J. Chem. Kinet.* **1990**, *22*, 1221.
(23) Czarnowski, J. *J. Chem. Soc. Perkin Trans. 2* **1991**, 1459.
(24) Wenger, J. C.; Le Calvé, S.; Sidebottom, H. W.; Wirtz, K.; Martín Reviejo, M.; Franklin, J. A. *Environ. Sci. Technol.* **2004**, *38*, 831.
(25) NIST Chemistry WebBook, NIST Standard Reference Database Number 69, http://webbook.nist.gov/chemistry/, 2011.
(26) Evaluated Kinetic Data for Atmospheric Chemistry. IUPAC Subcommittee for Gas Kinetic Data Evaluation. http://www.iupac-kinetic.ch.cam.ac.uk, 2011.